LETTER

doi:10.1038/nature09427

Nonlinear electrophoresis of dielectric and metal spheres in a nematic liquid crystal

Oleg D. Lavrentovich[1], Israel Lazo[1] & Oleg P. Pishnyak[1]

Electrophoresis is a motion of charged dispersed particles relative to a fluid in a uniform electric field[1]. The effect is widely used to separate macromolecules, to assemble colloidal structures and to transport particles in nano- and microfluidic devices and displays[2–4]. Typically, the fluid is isotropic (for example, water) and the electrophoretic velocity is linearly proportional to the electric field. In linear electrophoresis, only a direct-current (d.c.) field can drive the particles. An alternating-current (a.c.) field is more desirable because it makes it possible to overcome problems such as electrolysis and the absence of steady flows[5,6]. Here we show that when the electrophoresis is performed in a liquid-crystalline nematic fluid, the effect becomes strongly nonlinear, with a velocity component that is quadratic in the applied voltage and has a direction that generally differs from the direction of linear velocity. The new phenomenon is caused by distortions of the liquid-crystal orientation around the particle that break the fore–aft (or left–right) symmetry. The effect makes it possible to transport both charged and neutral particles, even when the particles themselves are perfectly symmetric (spherical), thus allowing new approaches in display technologies, colloidal assembly and separation, microfluidic and micromotor applications.

The electric charge of a particle dispersed in a fluid is screened by a diffuse cloud of mobile ions, called counterions, with charges of sign opposite to that of the particle. When an electric field is applied, the counterions and the particle move in opposite directions. For a small particle, the electrophoretic velocity, $\mathbf{v}$, is determined by the electrostatic 'pulling' force proportional to the applied electric field, $\mathbf{E}$, and by the viscous drag force, as expressed by Smoluchowski's formula[1]:

$$\mathbf{v} = \mu\mathbf{E} \quad (1)$$

Here $\mu = \varepsilon_m\zeta/\eta$ is the electrophoretic mobility of the particle, ζ is the zeta potential characterizing the charge of the particle and its spatial distribution, ε_m is the dielectric permittivity of the medium and η is the medium's viscosity. According to equation (1), an a.c. field with a zero time average produces no net propulsion: a change in field polarity changes the sign of $\mathbf{v}$ and the period-averaged displacement is zero. This is why numerous applications of electrophoresis, ranging from translocation and separation of macromolecules[2] to controlled assembly of colloidal particles[3], microfluidics and displays[4], rely on d.c. driving. The latter represents a certain drawback as the d.c. field might lead to undesirable electrochemical reactions, and explains the strong interest in mechanisms with a nonlinear relationship between $\mathbf{v}$ and $\mathbf{E}$ (refs 5, 6). Most studies consider isotropic fluids as an electrophoretic medium, in which case the nonlinear behaviour can be observed either for high voltages or for particles with special properties, such as a patterned surface[6]. In the first case, the nonlinear correction is cubic, such that $v = \mu E + \mu_3 E^3$, where μ_3 is a nonlinear mobility; a non-zero μ_3 was found also in nematic liquid crystals[7].

We demonstrate a type of electrophoresis in an orientationally ordered fluid, a nematic liquid crystal, in which $\mathbf{v}(\mathbf{E})$ has a quadratic dependence on E. The dependence $v \propto E^2$ makes it possible to move particles even with a symmetric a.c. field with a modest amplitude, as the change in field polarity does not change v. The new phenomenon is caused by asymmetric distortions of liquid-crystal orientation around the particle. The electrophoretic velocities linear and quadratic in E generally have different directions, resulting in a high degree of freedom in moving the particle in space. We demonstrate electrophoretic motion parallel, antiparallel and perpendicular to $\mathbf{E}$, as well as motion along curvilinear tracks set by the spatially varying orientation of the liquid crystal.

We used a nematic liquid crystal E7 (EM Industries) that melts into an isotropic phase at $t_{NI} = 58\ ^\circ$C. Molecular orientation in liquid crystal is described by the director $\hat{\mathbf{n}}$; because the medium is nonpolar, $\hat{\mathbf{n}} = -\hat{\mathbf{n}}$ (that is, the two opposite directions are equivalent). A liquid-crystal layer of thickness $h = 50$–$80\ \mu$m between two glass plates is aligned uniformly along the x axis, $\hat{\mathbf{n}}_0 = (1, 0, 0)$, using layers of buffed polyimide. The electric field, $\mathbf{E} = (E, 0, 0)$, is parallel to the x axis. The dielectric anisotropy of E7, $\Delta\varepsilon = \varepsilon_{||} - \varepsilon_\perp = 13.8$, is positive ($\varepsilon_{||}$ and $\varepsilon_\perp$ are the dielectric permittivities for $\mathbf{E}$ parallel and perpendicular to $\hat{\mathbf{n}}$, respectively), such that $\mathbf{E}$ does not influence $\hat{\mathbf{n}}$ away from the particles. Two aluminium strips separated by a gap $L = 5$–12 mm served as the electrodes.

We used dielectric spheres, of diameter $2a = 5$–$50\ \mu$m, made of silica (Bangs Laboratories), borosilicate and soda lime glass (Duke Scientific), as well as gold spheres with $2a = 5.5$–$9\ \mu$m (Alfa Aesar). To ensure the perpendicular orientation of $\hat{\mathbf{n}}$ at the particle's surface, the gold spheres were etched with an acid and the dielectric spheres were functionalized with octadecyltrichlorosilane (OTS) or *N*,*N*-didecyl-*N*-methyl-(3-trimethoxysilylpropyl) ammonium chloride (DDMAC), both purchased from Sigma-Aldrich.

Ionic impurities make the voltage profile across the liquid-crystal cell time dependent. To screen the field, the ions move and build electric double layers near the electrodes, within a characteristic time[8] $\tau_e = \lambda_D L/2D \approx 1$–$3$ min, where $\lambda_D = 0.1$–$1\ \mu$m is the Debye screening length and $D = 10^{-10}$–$10^{-11}\ m^2\,s^{-1}$ is the diffusion coefficient. We measure $\mathbf{v}$ within a few minutes of voltage application, in the regime of stationary motion. Then the voltage polarity is reversed and $\mathbf{v}$ is measured again.

In the isotropic melt, the dielectric spheres show a classic linear electrophoresis (Fig. 1a) similar to the observations of ref. 9, which were made for both the isotropic melt and an unaligned liquid crystal. The gold spheres do not move: $\mu^I_{Au} = 0$.

Once the material has cooled into the nematic phase, each particle generates a radial director configuration in its immediate vicinity. To match the overall uniform alignment of the liquid crystal, each sphere acquires a satellite topological defect: either a point defect, the so-called hyperbolic hedgehog[10] (Fig. 1d), or an equatorial disclination ring[11]. The pair hedgehog–sphere represents an elastic dipole[10], $\mathbf{p} = (p_x, 0, 0)$, that is elastically repelled from the bounding plates of the cell. The particles levitate in the bulk[12], thus resisting sedimentation, which hinders electrophoresis in isotropic fluids[13]. If there is no field, the levitating spheres experience Brownian motion with zero net displacement.

Once the d.c. field has been applied, the spheres with dipolar configurations demonstrate strongly nonlinear electrophoresis (Fig. 1a, b, c) with the velocity-field dependence

[1]Liquid Crystal Institute and Chemical Physics Interdisciplinary Program, Kent State University, Kent, Ohio 44242, USA.

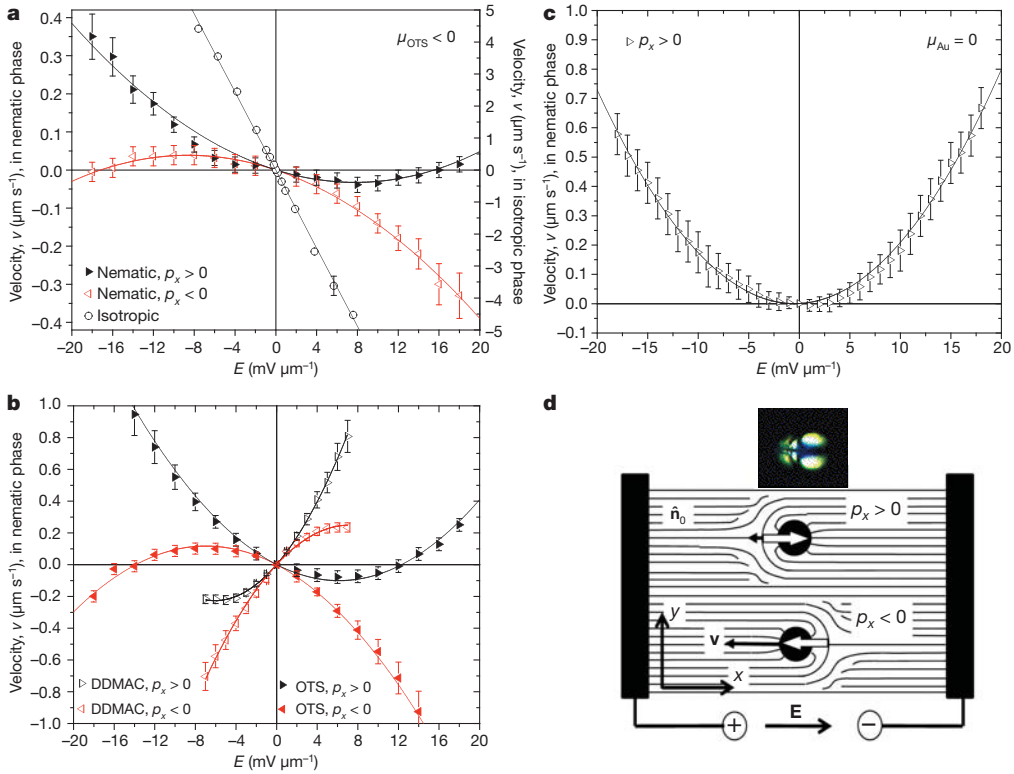

Figure 1 | Nonlinear electrophoresis in a d.c. field. Electrophoretic velocity versus applied field for OTS-coated silica spheres ($2a = 5.08\,\mu m$) in the isotropic phase (65 °C) and in the nematic phase (25 °C) of E7 with two polarities of the elastic dipole (**a**); for negatively charged OTS-coated borosilicate spheres ($2a = 9.6\,\mu m$) and positively charged DDMAC-coated borosilicate spheres ($2a = 17.3\,\mu m$) in the nematic phase (**b**); and for neutral gold spheres ($2a = 10\,\mu m$) in the nematic phase (**c**). **d**, Scheme of experiment with **E** parallel to $\hat{\mathbf{n}}_0$; the hyperbolic hedgehog is either on the left-hand side of the sphere ($p_x > 0$) or the right ($p_x < 0$). Inset, polarizing microscope image of a glass sphere with $2a = 50\,\mu m$ and $p_x > 0$. Error bars, s.d. taken for over 100 particles.

$$v = \mu E + \beta E^2 \qquad (2)$$

For neutral gold particles, $\mu^N_{Au} = 0$ and the dependence of v on E is parabolic, with $\beta^N_{Au} = 2 \times 10^{-3}\,\mu m^3\,mV^{-2}\,s^{-1}$ (Fig. 1c). For dielectric particles, both μ and β are non-zero; for example, $\mu^N_{OTS} = -0.03\,\mu m^2\,mV^{-1}\,s^{-1}$ and $\beta^N_{OTS} = 2.55 \times 10^{-3}\,\mu m^3\,mV^{-2}\,s^{-1}$ for $2a = 9.6\,\mu m$, and $\mu^N_{DDMAC} = 0.07\,\mu m^2\,mV^{-1}\,s^{-1}$, $\beta^N_{DDMAC} = 5.5 \times 10^{-3}\,\mu m^3\,mV^{-2}\,s^{-1}$ for $2a = 17.3\,\mu m$. The non-zero quadratic term in equation (2) means that the electrophoresis in the liquid crystal can be naturally induced by an a.c. field, as confirmed experimentally (Fig. 2 and Supplementary Fig. 1).

Equation (2) is written for the case in which the vectors **v**, **p** and **E** are all parallel (or antiparallel) to the x axis (Fig. 1d). Generally, the dependence of **v** on **E** involves tensorial coefficients that depend on **p**, such that the components of the velocity, v_i, and the field, E_j ($i, j = x, y, z$), are related as follows:

$$v_i = \mu_{ij} E_j + \beta_{ijk} E_j E_k \qquad (3)$$

The tensor character of the dependence of **v** on **E** is manifested by the fact that β (but not μ) changes sign with **p**, such that the velocity components originating in the linear ($\mu_{xx}E_x$) and quadratic ($\beta_{xxx}E_x^2$) parts of equation (3) can be not only parallel but also antiparallel to each other (Figs 1a, b and 2a, b, d; see also Supplementary Movie 2b, d). Another illustration comes from the experiments with the liquid crystal MLC7026-000 (Merck), in which $\Delta\varepsilon = -3.7$. We apply the field $\mathbf{E} = (0, 0, E_z)$ perpendicularly to $\mathbf{p} = (p_x, p_y, 0)$ (using transparent electrodes at the glass plates); because $\Delta\varepsilon < 0$, the field does not perturb the liquid crystal far from the particles. By buffing the polyimide aligning layer in a circular fashion, we prepared a cell in which $\hat{\mathbf{n}}_0(x,y)$ formed a 'race-track' configuration (Fig. 3). The spheres moved in the x–y plane of the cell, perpendicular to **E**, either anticlockwise or clockwise around the track, depending on the polarity of **p** (Fig. 3).

In a separate experiment, we verified the role of dielectric anisotropy. In E7 it is large ($\Delta\varepsilon = 13.8$), causing a dielectric torque proportional to $\Delta\varepsilon$ on the director near the spheres. To minimize this torque, we mixed E7 with MLC7026-000; $\Delta\varepsilon$ decreases to 1.25 at a 18.7 wt% concentration of E7, and almost vanishes ($\Delta\varepsilon = 0.03$) at 13.45 wt% (measured at 25 °C and 1 kHz). The electrophoresis in these two mixtures was similar to that in E7 (Fig. 2c), demonstrating that the dielectric reorientation of $\hat{\mathbf{n}}$ is not the prevailing driving mechanism.

The a.c. electrophoresis and nonlinear d.c. electrophoresis are observed for spherical particles when the director distortions around them are of a dipolar type (Fig. 1d). If the director distortions preserve the fore–aft symmetry, as is the case for the equatorial defect ring (Fig. 4a), these effects vanish. To produce the defect structure with an equatorial ring, we followed a procedure from ref. 14, using shallow cells with a separation between the plates that is close to the diameter of the particles. The a.c. field caused back-and-forth linear electrophoresis of the particles but no net propulsion.

The experiments suggest that the a.c. and nonlinear d.c. electrophoresis mechanisms are rooted in the nature of the director distortions of the liquid-crystal carrier medium. In an isotropic fluid, the broken symmetry of the particles can lead to nonlinear d.c. and a.c. electrophoresis[15–17] with $v \propto E^2$, as reviewed in refs 13, 15, in the second of which the term 'induced-charge electrophoresis' (ICEP) was introduced. ICEP was experimentally demonstrated for anisotropic quartz particles[16] and for Janus spherical particles in an isotropic fluid[17]. The important difference of liquid-crystal electrophoresis is that the motion is caused by the broken symmetry of the medium rather than of the particle (Fig. 4).

Consider an uncharged metallic (gold) sphere in a liquid crystal. Once the field is on, the mobile ions of liquid crystal move in opposite directions. These ions cannot penetrate the particle and thus accumulate

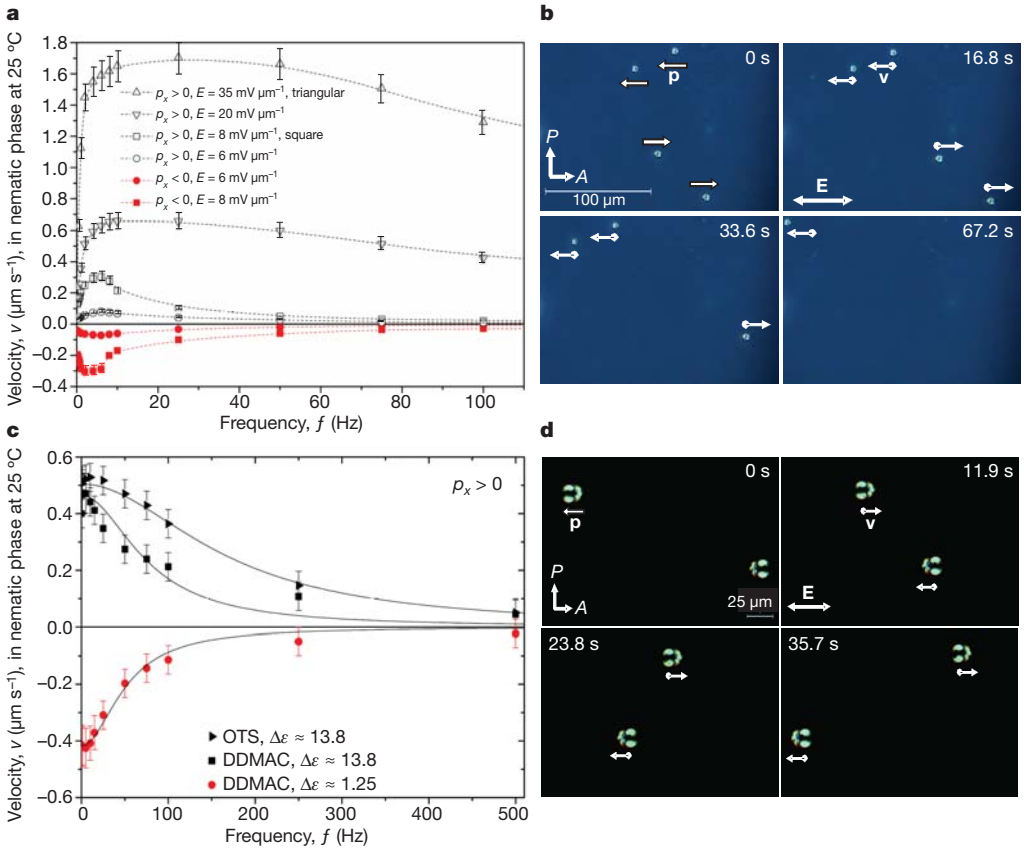

Figure 2 | A.c. electrophoresis in the nematic liquid crystal. **a**, OTS-coated silica particles ($2a = 5.08$ μm) driven by triangular and square a.c. pulses. The lines are guides for the eye. **b**, Optical microscope textures of particles viewed between a crossed polarizer (P) and analyser (A) at times 0, 16.8, 33.6 and 67.2 s after the triangular-pulse a.c. field (45 mV μm^{-1}, 100 Hz) is applied. **c**, DDMAC-treated borosilicate particles ($2a = 17.3$ μm) driven by a sinusoidal field (10 mV μm^{-1}) in E7 (squares); the same particles in the same field, but now moving in a mixture with 18.7 wt% of E7 (circles); and OTS-treated silica particles ($2a = 5.08$ μm) in a sinusoidal field (20 mV μm^{-1}) in E7 (triangles). The solid curves represent the fits from equation (4). **d**, As in **b**, but for DDMAC-treated particles ($2a = 17.3$ μm) in a mixture with 13.5 wt% of E7 0, 11.9, 23.8 and 35.7 s after a field (30 mV μm^{-1}, 1 Hz) is applied. The movie versions of **b** and **d** are available in the Supplementary Information. Error bars, s.d. taken for over 100 particles.

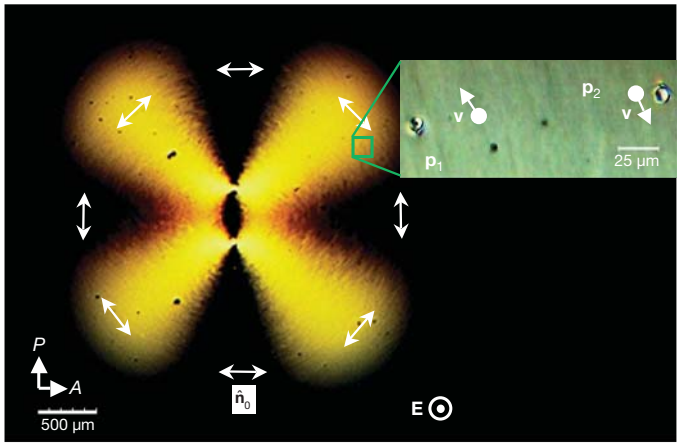

Figure 3 | Electrophoretic motion of DDMAC-coated borosilicate spheres. Particles with $2a = 9.6$ μm moving in the plane perpendicular to the electric field, along the 'race-track' trajectories set by a non-uniform director $\hat{\mathbf{n}}_0$.

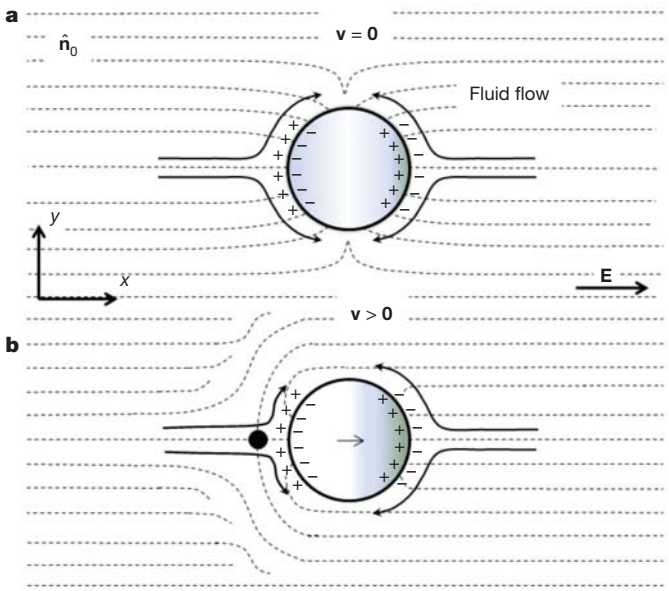

Figure 4 | Spherical particles with normal anchoring in a nematic liquid crystal with quadrupolar or dipolar symmetry of director distortions. The Saturn ring (**a**, quadrupolar) preserves the fore–aft symmetry and results in zero electrophoretic mobility; the hyperbolic hedgehog (**b**, dipolar) breaks the fore–aft symmetry and is responsible for the nonlinear electrophoresis.

at its opposite sides. The field-induced ionic clouds attract the 'image charges' from within the conducting sphere, producing a Debye screening layer. The field-induced zeta potential can be estimated[15] as $\zeta_{ind} \approx aE$. In the steady state, the tangential component of **E** drives the mobile ions and, thus, the fluid from the poles of the sphere towards its equator. The directionality of this ICEP flow does not change with field reversal (Fig. 4). If the particle and the surrounding medium have a mirror-image symmetry, the slip velocity produces no electrophoretic propulsion, as illustrated in Fig. 4a for a sphere with an equatorial defect ring. The hedgehog configuration (Fig. 4b) breaks this symmetry. The flows on the opposite sides of the sphere are not symmetric anymore, and give rise to an electrophoretic velocity that is proportional to the square of the field $v \propto (aE)E = aE^2$.

This qualitative picture suggests that in equation (2), $\beta = \delta\varepsilon_m a/\eta$ for the metallic particles and $\beta = \delta\varepsilon_d\lambda_D/\eta$ for the dielectric particles, where δ is the dimensionless factor characterizing the medium asymmetry; $\delta = 0$ in Fig. 4a and $\delta \neq 0$ in Fig. 4b. Using $2a = 10\,\mu m$, $\eta = 0.1$ Pa s (ref. 9), $\varepsilon_m = 10\varepsilon_0$ (ε_0, permittivity of free space), $\varepsilon_d = 5.8\varepsilon_0$, $\lambda_D = 1\,\mu m$ and $\delta = 1$, we find that $\beta = 5 \times 10^{-3}\,\mu m^3\,mV^{-2}\,s^{-1}$ for gold particles and that $\beta = 0.5 \times 10^{-3}\,\mu m^3\,mV^{-2}\,s^{-1}$ for the dielectric ones, values that are of the same order as the experimental ones.

It is of interest to consider how v depends on the frequency of the sinusoidal a.c. field (Fig. 2c), following the considerations for isotropic fluids[15,18,19]. The ICEP velocity is controlled by two timescales: a characteristic charging time, $\tau_c = \lambda_D a/D$ (for a conductive sphere) or $\tau_c = \varepsilon_m\lambda_D^2/\varepsilon_d D$ (for a dielectric sphere), and a characteristic electrode charging time, $\tau_e = \lambda_D L/2D$. These are of order of magnitude $\tau_c = 10^{-2}$ s and $\tau_e = 10^2$ s for $\lambda_D = 1\,\mu m$ and $D = 10^{-11}\,m^2\,s^{-1}$. For $\lambda_D \ll a \ll L$, the bulk a.c. field is controlled by τ_e:

$$E_0(t) = \frac{V_0}{L}\cos(\omega t)\mathrm{Re}\left(\frac{i\omega\tau_e}{1+i\omega\tau_e}e^{-i\omega t}\right)$$

The time-dependent polarization of the sphere is proportional to $\mathrm{Re}(e^{i\omega t}/(1+\omega\tau_c))$. The resulting frequency dependence

$$v(\omega) = v_0\frac{\omega^2\tau_e^2}{(1+\omega^2\tau_c^2)(1+\omega^2\tau_e^2)} \quad (4)$$

fits the experimental data for $v(f)$, where $f = \omega/2\pi$, very well (Fig. 2c). The velocity increases as ω^2 when ω is low, but for high ω v decreases because the ions cannot follow the rapidly changing field. All three experimental dependencies in Fig. 2c were fitted using equation (4) with almost the same parameter values, namely τ_c in the range 0.005–0.015 s, τ_e in the range 43–53 s and $L = 10$ mm.

Liquid-crystal electrophoresis is much richer than its isotropic counterparts. In an isotropic fluid the electrophoretic particle must be charged or be asymmetric, whereas in liquid-crystal electrophoresis the particle can be of any shape, such as a (highly symmetric) sphere, and can be of any charge (including zero). The components of velocity that originate in the linear and quadratic terms in equation (3) need not be parallel to each other and the particles can be moved in practically any direction in three-dimensional space. The phenomenon offers new perspectives for practical applications where highly flexible, precise and simple control of particle (or cargo) placement, delivery, mixing or sorting is needed. Examples include microfluidic devices and electrophoretic displays[20]. The practical potential of liquid-crystal-based electrophoresis is further increased by the fact that the trajectories and velocities of particles can be controlled not only by the frequency-dependent linear and quadratic mobilities in equations (2) and (3), but also by the spatially varying director field, $\hat{\mathbf{n}}_0(\mathbf{r})$.

Received 28 February; accepted 12 August 2010.

1. Russel, W. B., Saville, D. A. & Schowalter, W. R. *Colloidal Dispersions* (Cambridge Univ. Press, 1989).
2. Van Dorp, S., Keyser, U. F., Dekker, N. H., Dekker, C. & Lemay, S. G. Origin of the electrophoretic force on DNA in solid-state nanopores. *Nature* **5,** 347–351 (2009).
3. Hayward, R. C., Saville, D. A. & Aksay, I. A. Electrophoretic assembly of colloidal crystals with optically tunable micropatterns. *Nature* **404,** 56–59 (2000).
4. Comiskey, B., Albert, J. D., Yoshizawa, H. & Jacobson, J. An electrophoretic ink for all-printed reflective electronic displays. *Nature* **394,** 253–255 (1998).
5. Dukhin, A. S. & Dukhin, S. S. Aperiodic capillary electrophoretic method using an alternating current electric field for separation of macromolecules. *Electrophoresis* **26,** 2149–2153 (2005).
6. Bazant, M. Z., Kilic, M. S., Storey, B. D. & Ajdari, A. Towards an understanding of induced-charge electrokinetics at large applied voltages in concentrated solutions. *Adv. Colloid Interface Sci.* **152,** 48–88 (2009).
7. Ryzhkova, A. V., Podgornov, F. V. & Haase, W. Nonlinear electrophoretic motion of dielectric microparticles in nematic liquid crystals. *Appl. Phys. Lett.* **96,** 151901 (2010).
8. Ciuchi, F., Mazzulla, A., Pane, A. & Reyes, J. A. AC and DC electro-optical response of planar aligned liquid crystal cells. *Appl. Phys. Lett.* **91,** 232902 (2007).
9. Tatarkova, S. A., Burnham, D. R., Kirby, A. K., Love, G. D. & Terentjev, E. M. Colloidal interactions and transport in nematic liquid crystals. *Phys. Rev. Lett.* **98,** 157801 (2007).
10. Poulin, P., Stark, H., Lubensky, T. C. & Weitz, D. A. Novel colloidal interactions in anisotropic fluids. *Science* **275,** 1770–1773 (1997).
11. Kuksenok, O. V., Ruhwandl, R. W., Shiyanovskii, S. V. & Terentjev, E. M. Director structure around a colloidal particle suspended in a nematic liquid crystal. *Phys. Rev. E* **54,** 5198–5203 (1996).
12. Pishnyak, O. P., Tang, S., Kelly, J. R., Shiyanovskii, S. V. & Lavrentovich, O. D. Levitation, lift, and bidirectional motion of colloidal particles in an electrically driven nematic liquid crystal. *Phys. Rev. Lett.* **99,** 127802 (2007).
13. Gamayunov, N. I. & Murtsovkin, V. A. Motion of dispersed particles in a uniform alternating electric field. *Colloid J. USSR* **49,** 615–616 (1987).
14. Gu, Y. & Abbott, N. L. Observation of Saturn-ring defects around solid microspheres in nematic liquid crystals. *Phys. Rev. Lett.* **85,** 4719–4722 (2000).
15. Squires, T. M. & Bazant, M. Z. Induced-charge electro-osmosis. *J. Fluid Mech.* **509,** 217–252 (2004).
16. Murtsovkin, V. A. & Mantrov, G. I. Investigation of the motion of anisometric particles in a uniform variable electric field. *Colloid. J. USSR* **52,** 1081–1085 (1990).
17. Gangwal, S., Cayre, O. J., Bazant, M. Z. & Velev, O. D. Induced-charge electrophoresis of metallodielectric particles. *Phys. Rev. Lett.* **100,** 058302 (2008).
18. Simonov, I. N. & Shilov, V. N. Theory of low-frequency dielectric-dispersion of a suspension of ideally polarizable spherical-particles. *Colloid J. USSR* **39,** 775–783 (1977).
19. Ramos, A., Morgan, H., Green, N. G. & Castellanos, A. AC electric-field-induced fluid flow in microelectrodes. *J. Colloid Interface Sci.* **217,** 420–422 (1999).
20. Kumar, S. A. *et al.* Dielectrophoretic and electrophoretic force analysis of colloidal fullerenes in a nematic liquid-crystal medium. *Phys. Rev. E* **80,** 051702 (2009).

Supplementary Information is linked to the online version of the paper at www.nature.com/nature.

Acknowledgements We are grateful to L. Tortora for help with surface functionalization of the particles and discussions. The research was supported by NSF DMR 0906751.

Author Contributions Experimental strategy was designed by O.D.L. Initial d.c. and a.c. field experiments for dielectric spheres were performed by O.P.P. The d.c. and a.c. field experiments for dielectric and metallic spheres, experiments with non-uniform director and analysis of data were performed by I.L. The paper was written by O.D.L.

Author Information Reprints and permissions information is available at www.nature.com/reprints. The authors declare no competing financial interests. Readers are welcome to comment on the online version of this article at www.nature.com/nature. Correspondence and requests for materials should be addressed to O.D.L. (olavrent@kent.edu).